Science Translational Medicine
AAAS

stm.sciencemag.org/cgi/content/full/13/591/eabc8362/DC1

Supplementary Materials for

Robot-induced hallucinations in Parkinson's disease depend on altered sensorimotor processing in fronto-temporal network

Fosco Bernasconi, Eva Blondiaux, Jevita Potheegadoo, Giedre Stripeikyte, Javier Pagonabarraga, Helena Bejr-Kasem, Michela Bassolino, Michel Akselrod, Saul Martinez-Horta, Frederic Sampedro, Masayuki Hara, Judit Horvath, Matteo Franza, Stéphanie Konik, Matthieu Bereau, Joseph-André Ghika, Pierre R. Burkhard, Dimitri Van De Ville, Nathan Faivre, Giulio Rognini, Paul Krack, Jaime Kulisevsky*, Olaf Blanke*

*Corresponding author. Email: olaf.blanke@epfl.ch (O.B.); jkulisevsky@santpau.cat (J.K.)

Published 28 April 2021, *Sci. Transl. Med.* **13**, eabc8362 (2021)
DOI: 10.1126/scitranslmed.abc8362

The PDF file includes:

Other Supplementary Material for this manuscript includes the following:

(available at stm.sciencemag.org/cgi/content/full/13/591/eabc8362/DC1)

Movie S1 (.mp4 format). MRI robot.
Movie S2 (.mp4 format). Reports from patients with PD and PH after riPH.
Data file S1 (Microsoft Excel format). Raw data for experiments with less than 20 samples.

SUPPLEMENTARY MATERIALS

Materials and Methods

Participants

riPH in patients with PD

For every patient, the doses of anti-parkinsonian medication were converted to the levodopa equivalent daily dose (*76*). The severity of motor symptoms was assessed by the score at the Movement Disorders Society - Unified Parkinson Disease Rating Scale (MDS-UPDRS) - part III (*77*), in "ON" state. We also assessed for all the participants the apathy scale (*78*) and the risk for psychosis (Prodromal Questionnaire PQ-16 (*79*); which was divided in part I (hallucinations, and negative symptoms-like experiences), and part II (level of distress linked to the experiences). Hallucinations were assessed with a semi-structured interview adapted from the psychosensory hallucinations Scale (PSAS) for Schizophrenia and Parkinson's disease (*80*). Next to PH, we also inquired about other hallucinations possibly experienced by patients with PD, for example, passage hallucinations (corresponding to animal, person or indefinite object passing in the peripheral visual field), visual illusion and complex hallucinations (structured visual, auditory or tactile hallucinations) as well as delusional ideas.

riPH in patients with PD (asynchronous versus synchronous stimulation)

For this experiment, the participants consisted of patients with PD and the symptom of PH (PD-PH, n=13), patients with PD without the symptom of PH (PD-nPH, n=13), and age-matched healthy controls (HC, n=21). Demographic and clinical data are summarized in Table S2. Patients with cognitive impairments (defined as a MoCA score (*81*) lower than 24 (*82*), treated with neuroleptics, affected by other central

neurological co-morbidities, affected by psychiatric co-morbidities unrelated to PD, and patients with recent (< one month) changes in their medical treatment were not included in the experiment. The HC included in the experiment never experienced PH, did not suffer from a neurological or psychiatric disease, and had no objective sign of cognitive impairment.

riPH in patients with PD (sensorimotor delay dependency)

For this experiment, ten PD-PH and twelve PD-nPH participated. The same patients participated in the experiment mentioned above, two PD-PH and one PD-nPH could not participate because of fatigue and/or tremor. One PD-PH and one PD-nPH were excluded from the analysis because they performed less than 18 trials (corresponding to one session) before definitively interrupting the experiment, due to fatigue and/or excessive tremor.

Brain mechanisms of riPH in healthy participants using MR-compatible robotics

Pilot experiment in mock scanner

Prior to conducting the fMRI experiment, a pilot experiment in a mock scanner using the MR-compatible robot was conducted to test whether PH could be induced with this robotic system in the supine position. For this pilot experiment, 24 participants (16 females, mean age±SD: 24.6±2.8 years old) were tested. All participants had no history of neurological or psychiatric disorders. All participants were right-handed as assessed by the Edinburg Handedness Inventory (mean index: 81.0± 16.3 (SD) and range: 40-100). All participants provided written informed consent prior to the experiment.

The experiment was approved by the Cantonal Ethics Committee of Geneva (Commission Cantonale d'Ethique de la Recherche-CCER).

Functional connectivity analysis in cPH-network in patients with PD

For this experiment, data from thirty participants were analysed. All patients were prospectively recruited from a sample of outpatients regularly attending to the Movement Disorders Clinic at Hospital de la Santa Creu i Sant Pau (Barcelona) based on the fulfilling of MDS new criteria for PD with minor hallucinations (PD-PH) - sense of presence and/or passage hallucinations (n=15) - and without hallucinations (PD-nPH; n=15). Demographic data are summarized in Table S13. Informed consent to participate in the experiment was obtained from all participants. The experiment was approved by the local ethics committee. The same dataset has been previously used in (*24*). Patients were diagnosed by a neurologist with expertise in movement disorders. Each patient was interviewed regarding years of formal education, disease onset, medication history, current medications, and dosage (levodopa daily dose). Motor status and stage of illness were assessed by the MDS-UPDRS-III (*77*). The PD-PH and PD-nPH groups did not differ for age, disease duration, dopaminergic doses, motor severity, cognition, depression, anxiety, and apathy (Table S13).

Exclusion criteria were history of major psychiatric disorders, cerebrovascular disease, conditions known to impair mental status other than PD, and the presence of factors that prevented MRI scanning (for example, claustrophobia, MRI non-compatible prosthesis). Patients with focal abnormalities in MRI or non-compensated systemic diseases (for example, diabetes, hypertension) were also excluded. In patients with motor fluctuations, cognition was examined during the “on” state. All patients were on

stable doses of dopaminergic drugs during the 4 weeks before inclusion. Patients were included if the hallucinations remained stable during the 3 months before inclusion in the experiment. No patient had used or was using antipsychotic medication. All patients had normal or corrected-to-normal vision.

Presence and type of minor hallucinations were assessed using the Hallucinations and Psychosis item of the MDS-UPDRS Part I. Patients with a sense of presence and/or passage hallucinations at least weekly during the last month were categorized as minor hallucinations. Cognitive functions were assessed by the Parkinson's Disease-Cognitive Rating Scale (PD-CRS) (*58*). Apathy was assessed with the Starkstein Apathy Scale (*78*).

Experimental procedure

riPH in patients with PD (asynchronous versus synchronous stimulation)

Each patient with PD participated in the experiment at a similar time (10am), after having received their usual anti-parkinsonian medication and was in his/her "best ON" state for the whole duration of the experiment as well as the psychological and neuropsychological assessments (*79, 80*). To investigate the riPH in patients with PD (and HC), we used the same experimental setup and device as our previous research (*31*). The robotic stimulation was administered through a robotic system (*83*) that has previously been used to induce the PH and other bodily illusions in healthy participants (*31*). The experimental design consisted of factors Synchrony (synchronous/asynchronous), Side (most/less affected) and Group (PD-PH/PD-nPH).

riPH in patients with PD (sensorimotor delay dependency)

Each patient performed the task exclusively with the hand that was most affected by PD, and only after having participated to the *asynchronous versus synchronous stimulation* experiment (see above). HC did the task with their dominant hand. Each participant was asked to perform three sessions; each session consisted of 18 trials (3 repetitions per delay). In total, each delay was repeated 9 times. The overall experiment lasted approximately 20 minutes. Between each session, the participant could take a break according to his/her needs. One PD-PH patient performed longer sessions. In total, PD-PH completed 57.8 ± 16.9 (mean ± SD) trials, PD-nPH completed 45 ± 12.8 (mean ± SD) trials, and HC completed 53.3 ± 3.91 (mean ± SD) trials. No statistical difference across groups was observed (Welch two Sample t-test, two-tailed): PD-PH versus PD-nPH: $t(17) = 1.97$, p-value = 0.065; PD-PH versus HC: $t(-9) = 0.89$, p-value = 0.39.

Brain mechanisms of riPH in healthy participants using MR-compatible robotics

For this experiment, we used a MR-compatible robotic system composed of a front and a back robot to generate the sensorimotor conflicts (Fig.2A in the main text; *84*). The front-robot of the MR-compatible robot contained a carbon-fiber rod attached to a slider allowing the participant to move along two directions (Fig.2A in the main text) and measured the movements. Movements of the carbon-fiber rod were electronically translated into movements of the back-robot. The back-robot was composed of a roller that touched the participant's back with stroking and tapping movements (for the general performance of the robotic system see *84*). The back-robot's shape was adapted to the spatial dimensions of the scanner bore and a wooden mattress structure with a

central slit was designed to allow the contact part of the back-robot to touch the back of the participants. The performance of the robotic system was previously validated inside a 3T and 7T MR scanner with a phantom (*84*). Visual Studio 2013 interface (Microsoft) was used to control the robotic system.

The robotic system used in this study differed from the one used in the behavioral experiment mentioned above (*riPH in patients with PD*) and of Blanke and colleagues (*31*) in multiple aspects. First, the participants were in the supine position compared to the standing position. Secondly, due to the spatial constraints of the MR-environment, the movement of the participants were limited to the middle of the back and not the whole back and participants had less degrees of freedom: they could only move in X (along the body) and Z (towards the body) directions. These different aspects might have led to a decrease of intensity of the PH induction compared to the standing robot used in the previous experiment (*31*).

Pilot experiment in mock scanner: experimental procedure

For this experiment, we tested whether we could induce PH in supine position in a mock scanner using the MR robot (riPH). The Mock scanner (MRI Simulator, Psychology Software Tools, Inc.) mimicked the scanner environment as well as the noise of the echo-planar imaging sequence. Participants were asked to perform repetitive movements with their right hand and this operated the front-robot, the movements of which were translated to the back-robot that provided tactile feedback to our participants' backs. In two conditions, tactile feedback was delivered either synchronously with the participants' movements (synchronous control condition, sync) or with a delay (asynchronous condition, async) that was previously shown to induce

the PH in healthy participants (Movie S2). In a third condition (desynchronous condition, desync), movements of the back-robot consisted of a pre-recorded sequence. Each condition lasted for 3 minutes, was repeated once, and given in random order. After each condition, a questionnaire adapted from (*31*) was filled where participants were asked to rate their degree of agreement or disagreement on a Likert scale from 0 to 6.

fMRI experiment: additional conditions

In the main fMRI experiment in healthy participants, we also analysed fMRI data recorded in two control conditions that allowed us to control for two aspects of sensorimotor stimulation that are not related to PH and determined the brain regions that were commonly activated by either of the sensorimotor conditions (synchronous, asynchronous; Fig. S3A-B) versus the control conditions (motor, touch; Fig. S3C-D). In the motor control condition, participants were asked to repeatedly move the front-robot with their right hand but did not receive any tactile feedback on their back (Fig. S3C). In the touch control condition, participants received touch feedback on their backs, but were not performing any movement with their right hand (the back-robot was actuated by a previously recorded movement sequence) (Fig. S3D).

At the end of the scanning session, participants repeated 30 seconds of the conditions presented in a randomised order (asynchronous and synchronous conditions) and had to answer to a questionnaire, which included the first six questions of the mock scanner pilot experiment: “I felt as if I was touching my body”, “I felt as if I was touching someone else’s body”, “ I felt as if I had no body”, “I felt as if I had two right hands”, “I felt as if someone else was touching my body” and “I felt as if a presence or someone was behind me”. Participants were asked to indicate on a 7-point Likert scale, how strongly they felt the sensation described by each item (from 0=not at all, to 6=very strong).

Data analysis

riPH in patients with PD (sensorimotor delay dependency)

Movement analysis

To assess whether the spatio-temporal pattern of the movement could explain the difference in rating of the riPH among groups, we calculated: i) the Inter-poke-interval (time between the end of the touch on the back of poke *n* and the beginning of the following touch – poke *n+1*), ii) duration of the poke and iii) the spatial distance between poke *n* and poke *n+1*. Data were analysed with linear mixed effects models lme4 and lmerTest both R packages (*67, 68*). The significance of fixed effects was estimated with a permutation test (5000 iterations; predicted mean R package (*69*)).

Inter-poke-interval (ipi). To assess the temporal aspects of the sensorimotor integration we computed the ipi for each individual and for each trial independently. Models were performed on the ipi for each participant, with Groups (PD-PH versus PD-nPH; PD-PH versus HC as fixed effects, and random intercepts for the participant.

Poke duration. To assess a second temporal aspect of the sensorimotor integration we computed the duration of each poke, for each individual and for each trial independently. Models were performed on the duration for each participant, with Groups (PD-PH versus PD-nPH; PD-PH versus HC) as fixed effects, and random intercepts for the participant.

Spatial distance between pokes. To further investigate the spatial aspects of the sensorimotor integration we computed the Euclidean distance between pokes for each trial and participant. Models were performed on each distance values for each participant, with Groups (PD-PH versus PD-nPH and PD-PH versus HC) as fixed effects, and random intercepts for the participant.

Movement analysis for the fMRI task in healthy participants

To ensure that riPH were not due to any movement differences across experimental conditions, we calculated the total distance that each participant moved the front-robot.

Common PH-network for sPH and riPH

Lesion network mapping analysis

In order to assess the functional network derived from PH, we applied lesion network mapping (*48*). This method has the advantage of not requiring functional neuroimaging data from patients and of accounting for the possibility that symptoms may arise from remote brain regions connected to the lesioned brain region rather than the damaged area itself (*48, 72*). The PH-lesions reported by Blanke and colleagues (*31*) were used as seed regions of interest (ROIs) except one lesion which was covering the whole brain, resulting in eleven lesions for the analysis. Briefly, the MR brain scans of the

lesions were normalized to a smoothed T1 Montreal Neurological Institute space (MNI space) template and lesions were subsequently traced manually slice by slice on the normalised brain scan using MRIcron (https://www.nitrc.org/projects/mricron). These lesion maps were then co-registered to the same MNI space than the healthy participants from the Enhanced Nathan Kline Institute Rockland Sample using SPM12 toolbox (Wellcome Department of Cognitive Neurology, Institute of Neurology, UCL, London, UK) in Matlab (R2016b, Mathworks).

All patients included in the analysis had PH (9). 1 of 12 patients with neurological lesions reported a tactile hallucination and this patient's tactile hallucination was not reported in relation to the PH.

fMRI acquisition and data pre-processing

The data analysis and the pre-processing steps were performed using the Statistical Parametrical Mapping (SPM 12) (Wellcome Department of Cognitive Neurology, Institute of Neurology, UCL, London, UK, http://www.fil. ion.ucl.ac.uk/spm/) and the functional connectivity toolbox CONN (*73*) (v.18.a, http://www.nitrc.org/projects/conn) in Matlab.

fMRI acquisition and data pre-processing: ***riPH in healthy participants (fMRI)***

The imaging data was acquired with a 3T Siemens Magnetom Prisma MR scanner at Campus Biotech MR Platform (Geneva). The functional data were acquired using an Echo Planar Imaging (EPI) sequence with a full brain coverage (43 continuous slices, FOV=230mm, TR=2.5s, TE=30ms, flip angle=90°, in-plane resolution=2.5x2.5mm2,

slice thickness=2.5mm using a 64-channel head-coil) containing 320 volumes for the experimental runs and 160 volumes for the localizer runs. For each participant, an anatomical image was recorded using a T1-weighted MPRAGE sequence (TR=2.3s, TE=2.32ms, Inversion time=900ms, flip angle=8°, 0.9mm isotropic voxels, 192 slices per slab and FOV=240mm).

Slice timing correction and spatial realignment was applied to individual functional images. The anatomical image was then co-registered with the mean functional image and segmented into grey matter, white matter and cerebro-spinal fluid (CSF) tissue. Finally, the anatomical and the functional images were normalized to the MNI brain template. Functional images were then smoothed with a Gaussian kernel with full-width half-maximum of 6mm. Head motion was assessed based on framewise displacement (FD) calculation (*85*). All participants had a mean FD value inferior to 0.50mm (mean FD=0.12±0.05 mm). The two experimental runs were filtered with a high-pass filter at 1/300 Hz to remove low frequency confounds, while the two localizers were filtered with a high-pass filter at 1/100 Hz.

fMRI acquisition and data pre-processing: Lesion network mapping analysis

Resting state and T1-weighted structural data from 151 healthy participants obtained from the publicly available Enhanced Nathan Kline Institute Rockland Sample (*49*) was used. All participants were right-handed and aged between 19 to 40 years (83 females, mean age±SD: 25.8 ± 5.5 years old). Scans were acquired with a 3T Siemens Magneton TrioTim syngo. For the resting state data, a multiband EPI sequence was used (multiband factor = 4, 64 continuous slices, TR = 1.4 s, TE = 30 ms, flip angle = 65°, slice thickness = 2 mm) and 404 scans were collected. For each participant, an anatomical image was recorded using a T1-weighted MPRAGE sequence (TR = 1.9 s,

TE = 2.52 ms, Inversion time = 900 ms, flip angle = 9°, 1 mm isotropic voxels, 176 slices per slab and FOV = 250 mm).

The first four functional scans were discarded from the analysis to allow for magnetic saturation effects: the analysis was performed on the 400 remaining scans. Slice timing correction and spatial realignment were applied to individual functional images. The anatomical T1-weighted image was segmented into grey and white matter and CSF. The functional and anatomical scans were then normalized to the MNI space. Finally, the functional scans were spatially smoothed with a 5 mm full-width at half-maximum isotropic Gaussian kernel. The six realignment parameters and their first-degree derivatives were added in addition to the averaged signals of the white matter and cerebro-spinal fluid. Participants with excessive motion were excluded from the analysis, this comprised 25 participants which had a mean FD higher than 0.5mm and where more than 15% of scans were affected by movement. In total, 126 participants were included in the analysis. Then, fMRI data were bandpass-filtered in the range of 0.008-0.09Hz.

Lesion network mapping: control analysis

To exclude that the regions resulting from the lesion network mapping in patients with lesions causing PH are involved in hallucinations more generally, the same method was applied to a control group of eleven patients suffering from structured visual hallucination (VH) (*50*). The sPH-network was defined as those PH regions that were not overlapping with the visual hallucination derived network.

In addition, we determine whether the riPH-network was specifically connected to the lesions causing PH as opposed to the lesions causing VH. Therefore, for each of the 126 participants in the database, the regionally-averaged resting-state BOLD signal time

courses were extracted from each PH and VH lesion and riPH-network (Fig.2D-E in the main text) and were pairwise correlated (Fisher Z-transformed Pearson correlation) to establish the functional connectivity matrix. For each lesion location, we averaged the connectivity measures for the riPH-networks. Then, we compared statistically the connectivity between the two groups (PH versus VH) using two sample t-test.

Bootstrap analysis on the cPH-network

To confirm that the overlapping regions between the riPH-network and the sPH-network were consistent and that our results were robust, we performed an additional bootstrap analysis. In the bootstrap analysis, first we generated 19 datasets, by randomly selecting 20 participants (corresponding to 20% less data than the full sample size). Second, for each generated dataset we recomputed the second group analyses used to define the riPH-network (asynchronous > [motor + touch] ∩ synchronous > [motor + touch]). Third, for each newly generated riPH-network, we performed the overlap with the sPH-network derived from the neurological patients. For each generated dataset, we calculated the Dice coefficient for the overlap between the generated healthy participants' maps and the sPH-network derived from the neurological patients. The Dice coefficient was defined as the number of overlapping voxels divided by the average number of voxels in the two maps (riPH-network and sPH-network).

Functional connectivity analysis in cPH-network in patients with PD

MRI scans were acquired with a 3T Philips Achieva. T1 weighted scans were obtained using a MPRAGE sequence (TR = 500 ms, TE = 50 ms, flip angle = 8, field of view

[FOV] = 23 cm with in-plane resolution of 256 × 256 and 1mm slice thickness). Resting-state functional MRI images were collected using an 8-minute sequence (TR = 2000 ms, TE = 30 ms, flip angle = 78, FOV = 240 mm, slice thickness = 3 mm).

Functional images were corrected for slice time and motion, co-registered with a high-resolution anatomical scan, normalised into MNI space, resampled to 2 x 2 x 2 mm3, and smoothed with an 8 mm3 FWHM Gaussian kernel for each participant. To estimate the excessive movement, the mean FD during the scanning was estimated with the exclusion threshold of 0.5 mm. The groups did not differ by the movement over the scanning period ($t = 1.18$, $p = 0.12$ with the mean FD of 0.29 ± 0.15 mm and 0.23 ± 0.16 mm for PD-PH and PD-nPH groups respectively) and did not reach the excessive movement threshold. Following the standard pipeline for confound removal of the CONN toolbox, the individual time courses of the segmented white matter and CSF, the 6 motion parameters with rigid body transformations and their first-order derivatives were extracted and regressed out of the data. Regressions were performed for the entire time-series. The blood oxygenation level dependent (BOLD) signal data were passed through a band filter of 0.01-0.1 Hz. A whole-brain grey matter mask in MNI space restricted data analysis.

We favoured the analysis of resting state fMRI over performing the robotic stimulation within the MRI, because for patients with PD, performing long motor tasks (as required by the MRI to have a good signal to noise ratio) can be particularly tiring, and therefore exacerbating the tremor. Thus, the probability to have poor data quality and a high rate of patient willing to interrupt the experiment prematurely was too high.

Whole-brain connectivity

During first-level voxel-to-voxel analysis the estimation of voxel-to-voxel functional bivariate correlation coefficients matrix within each participant were computed. From this voxel-to-voxel correlation matrix, the intrinsic connectivity contrast (ICC) was established (*86*). The ICC characterizes the strength of the global connectivity pattern between each voxel and the rest of the brain (*87*). Briefly, the ICC is based on network theory's degree metric, which represents the number of voxels showing a correlation with each other voxel. Therefore, a whole-brain map is produced wherein the intensity of each voxel reflects the degree to which that voxel is connected to the rest of the brain. A greater ICC score represents greater average strength of the correlations in a given voxel. We compared PD-PH versus PD-nPH. The correction of $p<0.001$ voxel level uncorrected and $p<0.05$ FDR cluster level corrected were applied.

Patient classification based on functional connectivity in the cPH-network: control analysis

To assess that the prediction analyses were not biased by the algorithm used, we conducted an additional analysis using Random Forest (RF) as algorithm. As done with the LDA algorithm, we conducted a leave one out cross-validation procedure with a Random Forest (RF) algorithm (using Caret R packages). To ensure that the Kappa value was above chance we conducted a permutation test (5000 iterations). In each iteration, functional connectivity values were permuted between sub-groups and the cross-validation procedure was repeated.

Supplementary Figures

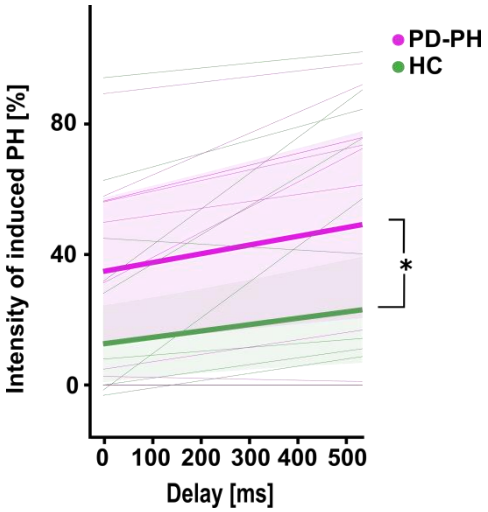

Fig. S1. riPH (patients with PD and HC). riPH in PD-PH depend on sensorimotor delay. The thicker lines indicate the mean of the fitted models, the thinner lines indicate the individual fit, and the shaded area indicates the 95% confidence interval.

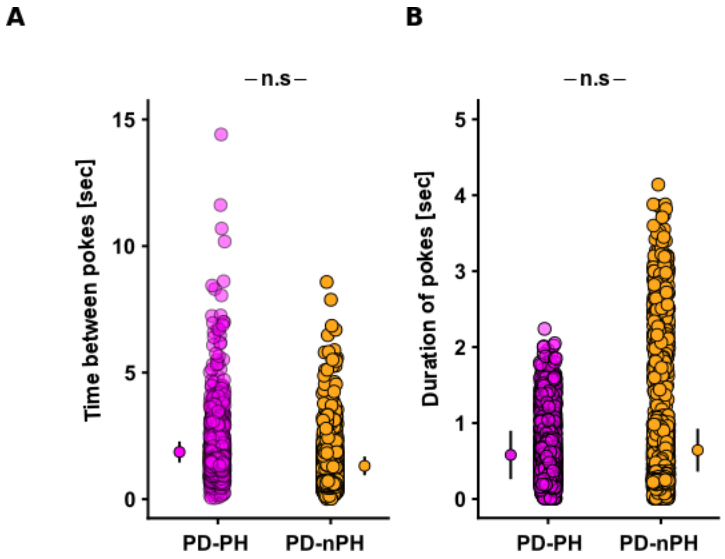

Fig. S2. Analysis of the movement patterns during the sensorimotor stimulation. A. Mixed effects linear regression between the time between pokes for PD-PH (purple) and PD-nPH (yellow). B. Mixed effects linear regression between duration of the pokes. Error bar represent 95% confidence interval. Each dot indicates the individual data for each trial and participants. The dot with the bar on the left and right side indicate the mixed effects linear regression. Error bar represents 95% confidence

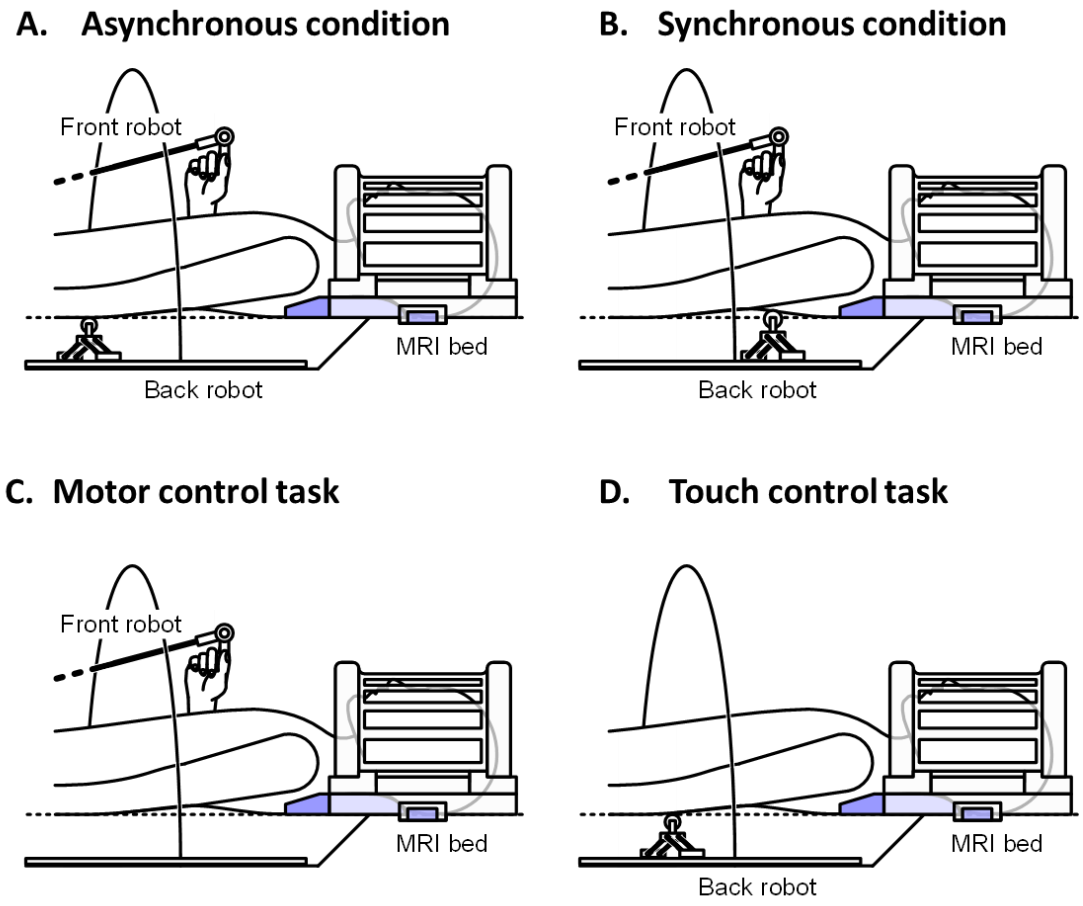

Fig. S3. The different conditions assessed with MR-compatible robotic system. The MR robotic system consisted of two parts: a front robot composed by a carbon fibre rod with which the participants performed the movement in 2 directions (X and Z) and a back robot that reproduced the movement of the front robot in the back of the participants. Different conditions were tested: (A) an asynchronous condition where the back robot was delayed of 500 ms compared to the front robot, (B) a synchronous condition in which no delay was introduced between the front robot and the back robot. In addition, in the fMRI experiment, two conditions were added: a motor control task, in which the participant was just performing the movements without any tactile feedback on the back (C) and a touch control task in which the participant only received the tactile feedback on the back without any movement (D). The contact part is composed of a roller effector that enables to touch the back of the participant. Two ultrasonic motors (USR60-E3NT, Shinsei) enable the effector to move. A home-made mattress was designed with an aperture to allow robotic stroking on the participant's back, while lying down.

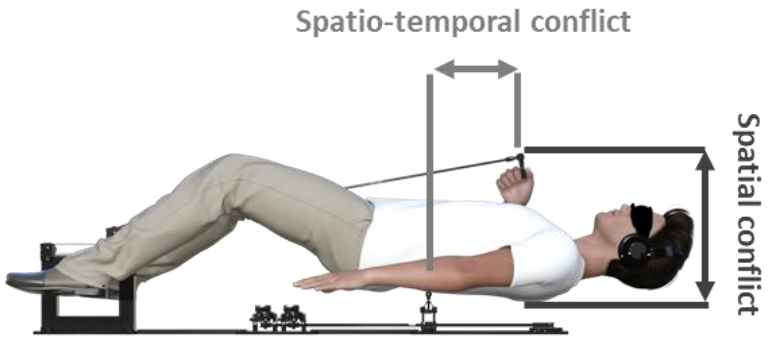

Fig. S4. Sensorimotor conflicts present in the robotic experiment. In the synchronous and in the asynchronous condition, a spatial conflict is present between the hand movement and the touch delivered on the back of the participants (indicated in grey). In the delayed asynchronous condition an additional spatio-temporal conflict is present since the movement performed by the hand is delayed and then delivered to the back of the participants.

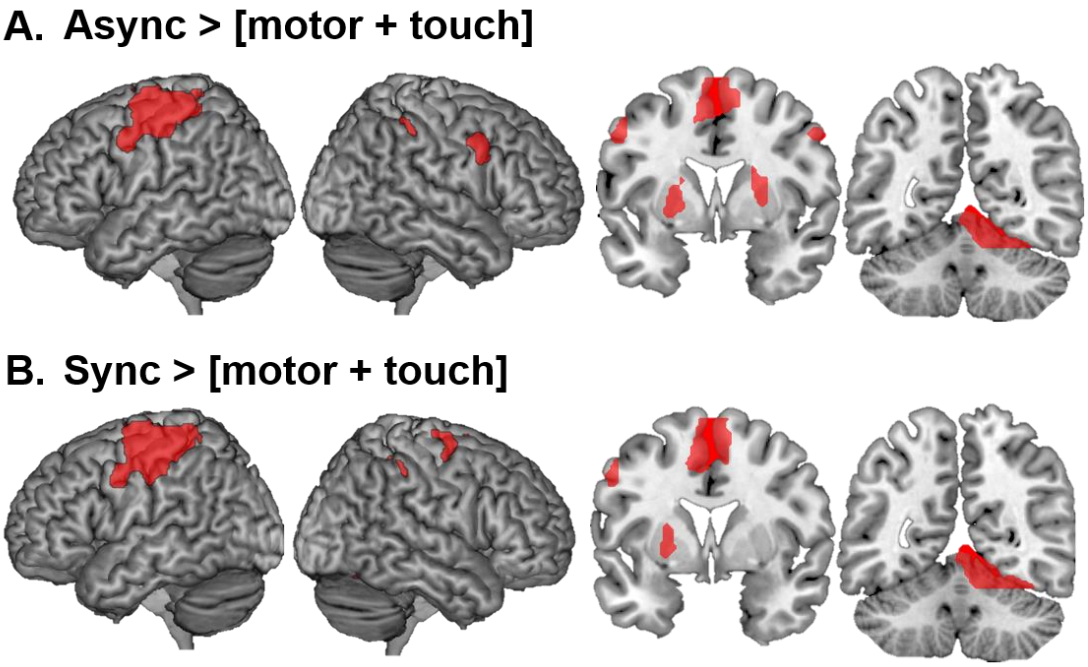

Fig. S5. riPH network. A. Brain regions reflecting the spatio-temporal sensorimotor conflict (async>[motor+touch]) revealing a large cortical-subcortical network including the left sensorimotor cortex (including adjacent parts of premotor cortex and superior parietal cortex), bilateral supplemental motor area (SMA) and adjacent parts of cingulate cortex, bilateral putamen, the right ventral premotor cortex, the right inferior parietal cortex (IPL) and the right cerebellum (Table S10). **B.** Brain regions responding to spatial sensorimotor conflict between the right-hand movement and the feedback on the back of the participants (sync>[motor+touch]).

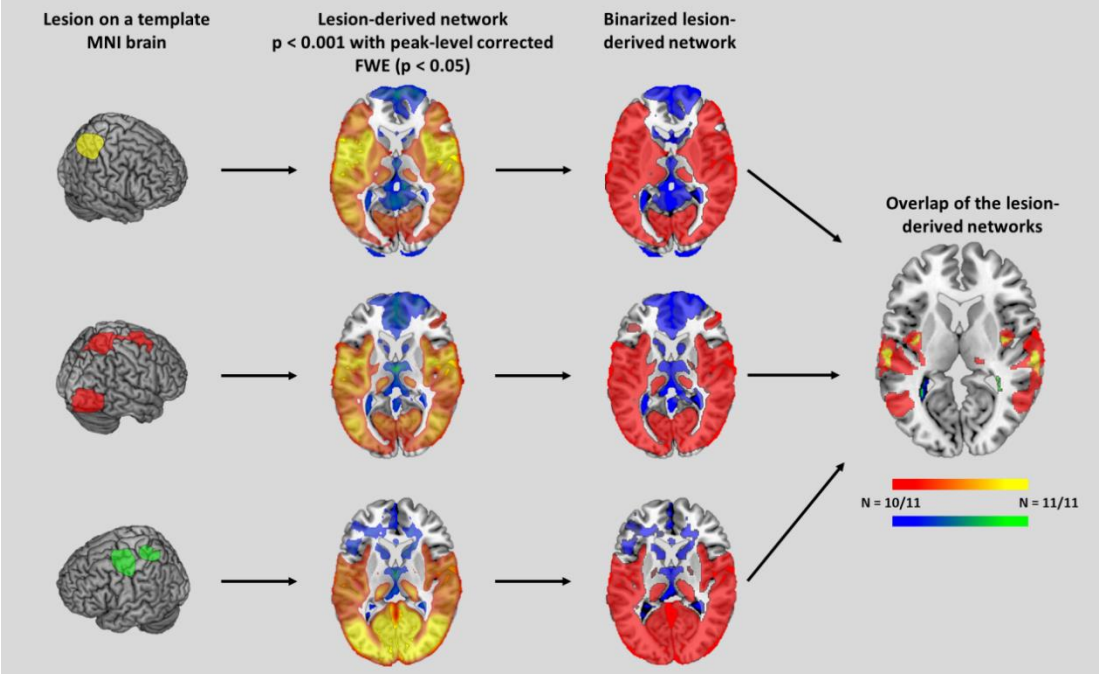

Fig. S6. Lesion network mapping analysis. The steps of the lesion network mapping analysis are shown: first the lesion is mapped to a template brain, then this lesion is used as a seed ROI in a resting state functional analysis performed on a normative database. The network obtained for each lesion is thresholded at $p < 0.001$ with peak-level corrected FWE ($p < 0.05$). All the lesions-derived networks are binarized and overlap to identify the regions functionally connected to most of the lesions.

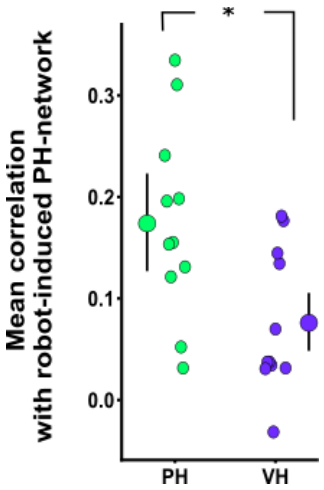

Fig. S7. Lesion connectivity with the riPH network. Lesions causing PH had greater functional connectivity with the riPH-network compared to VH lesions. * p-value<0.05.

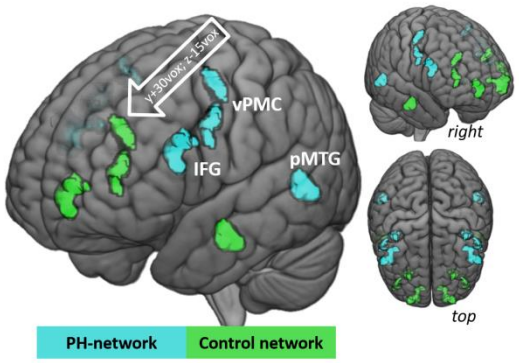

Fig. S8. Control regions for the resting-state fMRI analysis of patients with PD. Bilateral PH-network areas (red) shifted forward (green): Inferior frontal gyrus (IFG) x±20 y+30 z-15; ventral premotor cortex (vPMC) x±10 y+30 z-15; posterior middle temporal gyrus (pMTG) x y+30 z-15

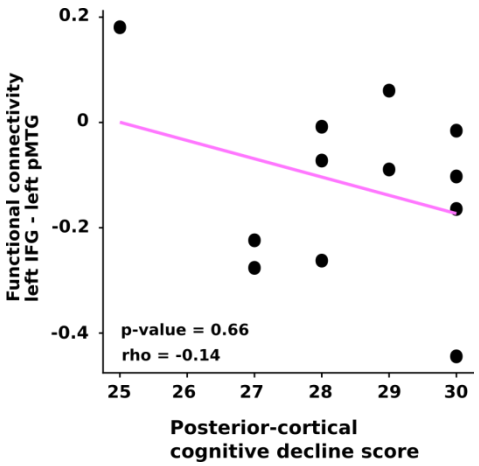

Fig. S9. Correlation between functional connectivity and posterior-cortical cognitive score. Correlation between the functional connectivity between left inferior frontal gyrus (IFG) and left posterior middle temporal gyrus (pMTG) and the posterior-cortical cognitive decline score in PD-PH.

Supplementary Tables

Table S1. Phenomenology of the sPH in PD.

	Number of patients	%
PH Valence		
• Positive/Neutral	7	54
• Negative	6	46
PH Gender		
• Female only	2	15
• Male only	1	8
• Both sex	2	15
• Undetermined	8	62
PH Lateralisation		
• Side only	6	46
• Back only	3	23
• Back and Side	2	15
• Front	1	8
• Other room	5	38
Occurrence (moment)		
• Day	3	23
• Night	4	31
• Anytime	6	46
Occurrence (place)		
• Home only	8	62
• Outside home only	0	0
• Both	6	46
Distance of PH		
• Less than 1m	5	38
• More than 1m	8	62

Table S2. Clinical variables for PD-PH and PD-nPH. The table shows the mean and standard deviation for several clinical and demographic variables.

	PD-PH (N = 13)	**PD-nPH (N = 13)**	***p-value***
Age	60.62 ± 13.19	65.69 ± 7.60	0.25
Gender	9 (M)	4 (M)	0.05 (χ2)
UPDRS-III	20.46 ± 12.08	19.15 ± 17.51	0.87
MoCA	26.85 ± 1.82	28.15 ± 1.57	0.08
PQ16	4.00 ± 2.00	0.69 ± 1.32	< 0.001
PQ16-2	3.54 ± 4.86	1.08 ± 2.63	0.1
Apathy	12.69 ± 8.06	10.23 ± 4.64	0.37
LEDD (mg/day)	727.77 ± 410.46	786.23 ± 653.28	0.8
Disease Duration (years)	9.46 ± 4.22	9.38 ± 5.72	0.5

Table S3. Clinical variables for PD-PH and HC. The table shows the mean and standard deviation for several clinical and demographic variables.

	PD-PH (N = 13)	**HC (N = 21)**	***p-value***
Age	60.62 ± 13.19	66.90 ± 5.75	0.06
Gender	9 (M)	11 (M)	0.9 (χ2)
MoCA	26.85 ± 1.82	28.52 ± 1.03	<0.001
PQ16	4.00 ± 2.00	0.24 ± 0.44	<0.001
PQ16-2	3.54 ± 4.86	0.00 ± 0.00	<0.001
Apathy	12.69 ± 8.06	6.33 ± 4.05	0.01

Table S4. Mean ratings for all questions and experimental conditions.

Question	Group	Synchrony	Side	Mean	Standard Deviation
PH	PD-PH	Async	Less affected side	1.67	2.31
PH	PD-PH	Async	Most affected side	2.23	2.17
PH	PD-PH	Sync	Less affected side	0.42	0.9
PH	PD-PH	Sync	Most affected side	1.31	1.93
PH	PD-nPH	Async	Less affected side	0.62	1.56
PH	PD-nPH	Async	Most affected side	0.23	0.83
PH	PD-nPH	Sync	Less affected side	0	0
PH	PD-nPH	Sync	Most affected side	0	0
PH	HC	Async	Less affected side	1.05	1.96
PH	HC	Async	Most affected side	1.33	2.15
PH	HC	Sync	Less affected side	0.52	1.66
PH	HC	Sync	Most affected side	0.86	1.93
Loss of agency	PD-PH	Async	Less affected side	1.83	2.25
Loss of agency	PD-PH	Async	Most affected side	2.25	2.14
Loss of agency	PD-PH	Sync	Less affected side	1.17	1.7
Loss of agency	PD-PH	Sync	Most affected side	1.75	1.71
Loss of agency	PD-nPH	Async	Less affected side	0.85	1.63
Loss of agency	PD-nPH	Async	Most affected side	0.54	0.97
Loss of agency	PD-nPH	Sync	Less affected side	0.08	0.28

Loss of agency	PD-nPH	Sync	Most affected side	0.23	0.6
Loss of agency	HC	Async	Less affected side	0.48	1.25
Loss of agency	HC	Async	Most affected side	0.81	1.47
Loss of agency	HC	Sync	Less affected side	0.24	0.89
Loss of agency	HC	Sync	Most affected side	0.9	1.7
Passivity experience	PD-PH	Async	Less affected side	2.33	2.31
Passivity experience	PD-PH	Async	Most affected side	3.08	2.43
Passivity experience	PD-PH	Sync	Less affected side	1.25	2.05
Passivity experience	PD-PH	Sync	Most affected side	2.08	2.14
Passivity experience	PD-nPH	Async	Less affected side	2.54	2.37
Passivity experience	PD-nPH	Async	Most affected side	1.77	2.05
Passivity experience	PD-nPH	Sync	Less affected side	1.54	2.22
Passivity experience	PD-nPH	Sync	Most affected side	1.38	1.94
Passivity experience	HC	Async	Less affected side	1.81	2.5
Passivity experience	HC	Async	Most affected side	3.29	2.31
Passivity experience	HC	Sync	Less affected side	1.29	2.22
Passivity experience	HC	Sync	Most affected side	2.33	2.61
Self-touch	PD-PH	Async	Less affected side	1.92	2.35
Self-touch	PD-PH	Async	Most affected side	1.38	1.66
Self-touch	PD-PH	Sync	Less affected side	2.08	2.27

Self-touch	PD-PH	Sync	Most affected side	3	2.24
Self-touch	PD-nPH	Async	Less affected side	0.85	1.57
Self-touch	PD-nPH	Async	Most affected side	0.85	1.57
Self-touch	PD-nPH	Sync	Less affected side	1.46	2.37
Self-touch	PD-nPH	Sync	Most affected side	1.92	2.56
Self-touch	HC	Async	Less affected side	2.38	2.69
Self-touch	HC	Async	Most affected side	1.86	2.46
Self-touch	HC	Sync	Less affected side	2.43	2.84
Self-touch	HC	Sync	Most affected side	2.81	2.84
PH front	PD-PH	Async	Less affected side	0	0
PH front	PD-PH	Async	Most affected side	0	0
PH front	PD-PH	Sync	Less affected side	0	0
PH front	PD-PH	Sync	Most affected side	0	0
PH front	PD-nPH	Async	Less affected side	0	0
PH front	PD-nPH	Async	Most affected side	0	0
PH front	PD-nPH	Sync	Less affected side	0	0
PH front	PD-nPH	Sync	Most affected side	0	0
PH front	HC	Async	Less affected side	0	0
PH front	HC	Async	Most affected side	0	0
PH front	HC	Sync	Less affected side	0	0
PH front	HC	Sync	Most affected side	0	0

Control	PD-PH	Async	Less affected side	0.25	0.62
Control	PD-PH	Async	Most affected side	0.54	1.2
Control	PD-PH	Sync	Less affected side	0.25	0.87
Control	PD-PH	Sync	Most affected side	0.38	0.96
Control	PD-nPH	Async	Less affected side	0	0
Control	PD-nPH	Async	Most affected side	0	0
Control	PD-nPH	Sync	Less affected side	0	0
Control	PD-nPH	Sync	Most affected side	0	0
Control	HC	Async	Less affected side	0.19	0.87
Control	HC	Async	Most affected side	0.19	0.87
Control	HC	Sync	Less affected side	0	0
Control	HC	Sync	Most affected side	0.24	1.09

Table S5. Statistical results for the ratings for all questions (from asynchronous versus synchronous stimulation) and experimental conditions. P-values are obtained from permutation statistics, unless indicated differently.

	Main effects			Interactions
PD-PH vs. PD-nPH (questionnaires ratings)	**Group**	**Synchrony**	**Side**	
I felt as if someone was close by	0.01	0.045	0.37	all > 0.05
I felt as if someone else was touching my back	0.38	0.1	0.41	all > 0.05
I felt as if I was touching my back	0.65	0.043	0.51	all > 0.05
I felt as if I was not controlling my movements or actions	0.045	0.26	0.76	all > 0.05
I felt as if I had two bodies (Control item 1)	0.26	0.98	0.88	all > 0.05
I felt someone was standing in front of me (Control item 2)	1	1	1	1
PD-PH vs. HC (questionnaires ratings)				
I felt as if someone was close by	0.48	0.033	0.38	all > 0.05
I felt as if someone else was touching my back	0.86	0.06	<0.01	all > 0.05
I felt as if I was touching my back	0.92	0.054	0.4	all > 0.05
I felt as if I was not controlling my movements or actions	0.073	0.6	0.28	all > 0.05
I felt as if I had two bodies (Control item 1)	0.79	0.85	0.71	all > 0.05
I felt someone was standing in front of me (Control item 2)	1	1	1	1

PD-PH vs. HC (spatial location of riPH)	**Side**	**Behind**	**Sum**	***p-value***	X^2
PD-PH	14	6	20	0.11	3.22
HC	2	14	16	<0.01	9
p-value (PD-PH vs. HC)	<0.01	0.12			
X^2	9	3.2			

Table S6. Statistical results for sensorimotor delay dependency, when comparing PD-PH and HC.
P-values are obtained from permutation statistics, unless indicated differently.

PH-PH vs. HC	***p-value***
riPH (sensorimotor delay dependency)	
Main effect of Group	0.046
Main effect of Delay	<0.001
Interaction Group*Delay	0.6

	PD-PH		**HC**		***p-value***
riPH (movement analyses)	mean	Standard Deviation	mean	Standard Deviation	
Duration poke	0.73	2.82	0.49	0.39	0.076
Distance between pokes	17.83	18.4	29.45	25-78	0.067
Inter-poke-interval	2.06	1.97	1.57	2.08	0.097

Table S7. Mean ratings for all questions used in the mock scanner experiment.

Question	Synchrony	Mean	Standard deviation
Self-touch	Desync	1.58	1.84
Self-touch	Async	2.08	2.10
Self-touch	Sync	2.54	2.48
I felt as if I was touching someone else's body	Desync	0.71	1.55
I felt as if I was touching someone else's body	Async	0.75	1.62
I felt as if I was touching someone else's body	Sync	0.50	1.29
Passivity experience	Desync	3.96	1.97
Passivity experience	Async	2.71	2.14
Passivity experience	Sync	1.67	1.97
PH	Desync	2.08	1.82
PH	Async	1.67	1.81
PH	Sync	0.67	1.55
Control (I felt as if I had no body)	Desync	0.67	1.09
Control (I felt as if I had no body)	Async	0.42	0.88
Control (I felt as if I had no body)	Sync	0.33	0.64
Control (I felt as if I had two right hands)	Desync	0.83	1.40
Control (I felt as if I had two right hands)	Async	0.75	1.51
Control (I felt as if I had two right hands)	Sync	0.63	1.06

Table S8. Mean ratings for all questions of the fMRI questionnaire.

Question	Synchrony	Mean	Standard deviation
Self-touch	Async	3.28	2.25
Self-touch	Sync	3.72	2.23
I felt as if I was touching someone else's body	Async	1.12	1.81
I felt as if I was touching someone else's body	Sync	0.88	1.59
Passivity experience	Async	3.40	2.25
Passivity experience	Sync	2.08	2.14
PH	Async	1.68	1.86
PH	Sync	1.04	1.65
Control (I felt as if I had no body)	Async	1.04	1.62
Control (I felt as if I had no body)	Sync	0.80	1.76
Control (I felt as if I had two right hands)	Async	0.56	1.33
Control (I felt as if I had two right hands)	Sync	0.36	0.76

Table S9. Spatiotemporal sensorimotor conflict PH regions. Regions activated during the contrast asynchronous > synchronous.

Regions	Voxels	BA	MNI coordinates			Peak level	Cluster-level
			x	y	z	t value	p value FWE
R. medial prefrontal cortex (mPFC)	770	8/9/32	5	41	47	6.2	0.001
R. inferior frontal gyrus (opercularis and triangularis) (IFG) / ventral premotor cortex (vPMC)	708	45/48	51	18	29	5.53	0.001
R. anterior insula (Ins)	566	47	36	24	-2	4.78	0.004
R. posterior middle temporal gyrus (pMTG)	479	37	54	-54	0	4.99	0.01

Table S10. Robotically induced brain activations.

Regions	*Voxels*	*BA*	*MNI coordinates*			*Peak level*	*Cluster-level*
			x	*y*	*z*	*t value*	*p value FWE*
Asynchronous > [motor + touch]							
L. Sensorimotor cortex (primary motor cortex (M1), primary somatosensory cortex (SI), supplemental motor area (SMA), middle cingulate cortex (MCC), Superior parietal lobe (SPL))	9894	2/3/4/6/40	-26	-16	58	7.93	p<0.001
R. Cerebellum	2840		11	-58	-14	7.99	p<0.001
R. Putamen / Globus pallidum	599		22	3	8	6.33	p<0.01
L. Putamen / Globus pallidum	560		-22	1	5	6.07	p<0.01
R. Inferior parietal lobe/supramarginal gyrus (SMG)	503	2/40	41	-37	47	4.1	p<0.01
R. ventral premotor cortex	357	6	55	8	38	5.58	p<0.05
Synchronous > [motor + touch]							
L. Sensorimotor cortex (primary motor cortex (M1), primary somatosensory cortex (SI), supplemental motor area (SMA), middle cingulate cortex (MCC), Superior parietal lobe (SPL))	12843	2/3/4/6/40	-25	-18	57	8.85	p<0.001
R. Cerebellum	3057		12	-57	-14	8.17	p<0.001
R. Inferior parietal lobe/supramarginal gyrus (SMG)	600	2/40	40	-34	45	4.8	p<0.01
L. Putamen / Globus pallidum	449		-22	0	5	7.34	p<0.05
R. Superior frontal gyrus / dorsal premotor cortex	385	6	28	-8	65	4.62	p<0.05
Conjunction between the asynchronous > [motor + touch] ∩ synchronous > [motor + touch]							
L. Sensorimotor cortex (primary motor cortex (M1), primary somatosensory cortex (SI), middle cingulate cortex (MCC), Superior parietal lobe (SPL))	12026	2/3/4/6/40	-26	-18	57	9.99	p<0.001
Supplemental motor area (SMA)		6	-5	-6	56	8.32	p<0.001
R. Cerebellum	2687		11	-57	-14	9	p<0.001
R. Inferior parietal lobe/supramarginal gyrus (SMG)	593	2/40	40	-34	45	4.59	p<0.01
L. Putamen / Globus pallidum	517		-23	0	4	6.44	p<0.01

Table S11. sPH-derived network. Brain areas that showed positive and negative correlation with most of the lesions (100% or 90% of overlap). Regions in the white matter were not reported.

Regions	*Overlap*	*Hemisphere*	*Voxels*	*BA*	*MNI coordinates*		
					x	*y*	*z*
Positive correlation							
Superior temporal gyrus (STG)	11	Right	770	22	62	25	13
	11	Left	582	22	-58	-29	13
Insula	11	Right	124	48	37	-6	12
	11	Left	135	48	-37	-7	9
	11	Left	81	48	-35	-9	-8
Postcentral sulcus	11	Left	111	48	-58	-16	19
Middle cingulate cortex (MCC)	11	Right	53		9	-11	38
	11	Left	100		-9	-11	37
Inferior frontal operculum/ ventral premotor cortex (vPMC)	11	Right	86	45/48	42	17	23
Temporo-parietal junction (TPJ): STG, MTG (only right), supramarginal gyrus (SMG), vPMC	10	Right	7153	21/22/48	56	-18	18
	10	Left	5318	21/22/48	-52	-16	16
Fusiform area	10	Right	2842	19/37	37	-52	-16
	10	Left	2916	19/37	-36	-53	-15
Middle temporal gyrus (MTG)	10	Left	1292	37	-48	-62	11
Dorsal premotor cortex (dPMC)	10	Right	370	6	44	-5	53
	10	Left	308	6	-40	-8	51
Amygdala	10	Right	295	36	29	3	-24
	10	Left	112	36	-26	2	-26
Thalamus	10	Right	126		15	-25	2
	10	Left	120		-12	-27	-2
Cerebellum	10	Left	107		-10	-65	-46
Hippocampus	10	Rigth	70		23	-36	-2
	10	Left	90		-20	-37	-1
Putamen	10	Right	69		36	-10	-8
Cuneus	10	Right	68	18	17	-70	26
	10	Left	68	18	-14	-72	22
Supplemental motor area (SMA)/Superior frontal gyrus	10	Left	58	6	-18	-8	68
Negative correlation	10						
Caudate	10	Right	70		17	-13	27

Table S12. VH-derived network. Brain areas that showed positive correlation with 90 % of the VH lesion locations (only the regions in the grey matter are reported). There was no overlap for all the lesions.

Regions	*Overlap*	*Hemisphere*	*Voxels*	*BA*	*MNI coordinates*		
					x	*y*	*z*
Positive correlation							
Superior temporal cortex and TPJ	10	Right	734	22/48	60	-14	9
	10	Left	148	42/22	-61	-32	14
	10	Left	147	22	-59	-9	-8
	10	Left	92	48	-51	-21	5
Middle and superior occipital cortex/ Inferior parietal lobule	10	Left	326	39/19	-38	-70	28
Hippocampus/parahippocampus	10	Left	118	20	-27	-31	-14
Thalamus/lingual area	10	Left	108	27	-14	-30	-2
Precentral cortex (dPMC)	10	Right	74	6	53	-3	44
	10	Left	51	6	-45	-7	51

Table S13. Clinical variables for PD-PH and PD-nPH. The table shows the mean and standard deviation for several clinical and demographic variables.

	PD-PH (N = 15)	**PD-nPH (N = 15)**	***p-value***
Age	70.93 ± 5.75	65.87 ± 7.52	0.06
Gender	9 (M)	10 (M)	0.7 ($\chi 2$)
MoCA	25.33 ± 3.06	24.00 ± 4.38	0.3
PD-CRS	91.53 ± 15.46	94.20 ± 15.81	0.67
PD-CRS (frontal)	62.87 ± 14.83	65.73 ± 15.26	0.62
PD-CRS (posterior)	28.67 ± 1.5	28.47 ± 1.68	0.83
UPDRS III	21.73 ± 8.91	25.60 ± 8..91	0.2
LEDD (mg/day)	722.13 ± 285.13	581.00 ± 310.49	0.2
Dopamine agonists (mg/day)	151.27 ± 122.82	143.4 ± 140.57	0.9
Disease Duration (years)	5.33 ± 3.74	3.73 ± 2.19	0.2

Table S14. Patients' classification based on functional connectivity and linear discriminant analysis algorithm. Contribution of each connectivity to the classification of PD-PH (versus PD-nPH), using LDA algorithm. The area under the ROC curve for each predictor is shown, with the variable with the highest score (left IFG - left pMTG) being the one giving the best prediction and contributing most to the model (*76*).

Connections	Variable Importance
Left-IFG - Left pMTG	0.81
Left pMTG - Right vPMC	0.78
Left IFG - Right vPMC	0.75
Left pMTG - Right pMTG	0.72
Left IFG - Right pMTG	0.7
Left IFG - Left vPMC	0.61
Right IFG - Right vPMC	0.6
Right pMTG - Right vPMC	0.6
Left pMTG - Left vPMC	0.6
Right IFG - Right pMTG	0.57
Right pMTG - Left vPMC	0.56
Left vPMC - Right vPMC	0.56
Left IFG - Right IFG	0.55
Right IFG - Left vPMC	0.54
Right IFG - Left pMTG	0.5

Table S15. Patients' classification based on functional connectivity and RF algorithm. Contribution of each connectivity to the classification of PD-PH (versus PD-nPH), using Random Forest algorithm. The importance of each variable to the model prediction accuracy is estimated by calculating the difference between the prediction accuracy on the out-of-bag portion of the data and the prediction accuracy after permuting each predictor variable. The difference in accuracy is then averaged over the trees used in the model and normalized by the standard error (*76*).

Connections	Variable Importance
Left-IFG - Left pMTG	3.23
Right IFG - Right vPMC	1.1
Left IFG - Right vPMC	0.93
Left IFG - Right pMTG	0.44
Left pMTG - Right vPMC	0.21
Left pMTG - Right pMTG	0.17
Right pMTG - left vPMC	0.14
Left vPMC - Right vPMC	0.13
Right IFG - Left vPMC	0.12
Right pMTG - Right vPMC	0.08
Right pMTG - Left vPMC	0.05
Left IFG - Left vPMC	0.05
Right IFG - Right pMTG	0.05
Left IFG - Right IFG	0.05
Right IFG - Left pMTG	0.03